

COMPUTER-SIMULATED TRANSIENT EVOLUTION OF 1.55 $\mu$ m  
LASER SPECTRA

M. Osinski\* and M.J. Adams\*\*

Department of Electronics, University of Southampton,  
Southampton, SO9 5NH, Hampshire, UK.\* On leave from Institute of Physics, Polish Academy  
of Sciences, Warsaw, Poland.\*\* Now at British Telecom Research Laboratories,  
Martlesham Heath, Suffolk.Résumé

Le comportement transitoire du spectre des lasers émettant à la longueur d'onde 1.55 $\mu$ m a été calculé numériquement en résolvant les équations cinétiques (rate equations) multimodes dans lesquelles l'effet de l'émission spontanée couplée dans chaque mode a été incorporé. On a utilisé un modèle analytique simple pour le spectre de gain qui suppose la recombinaison entre des bandes paraboliques sans règles de sélection de k. Les résultats montrent des oscillations de relaxation rapides dans chaque mode ainsi que les effets de la compétition entre les modes qui se déroule plus lentement. La distribution de l'intensité et la compétition parmi les modes sont déterminées principalement par le décalage en longueur d'onde entre le sommet de la courbe de gain à l'état stationnaire et le mode Fabry-Pérot le plus proche. Les oscillations de relaxation et la compétition inter-modale sont illustrées à l'aide d'un ciné-film 16 mm sous une forme permettant la compréhension intuitive des effets de l'évolution temporelle.

Abstract

The transient evolution of 1.55  $\mu$ m-wavelength laser spectra has been calculated from numerical solution of the multimode rate equations including the effects of spontaneous emission into the modes. A simple analytical model for gain spectrum has been used which assumes recombination between parabolic bands with no k-selection. The results show the characteristic relaxation oscillations in each mode together with competition effects between the modes which occur with a rather slower time scale. The principal parameter which determines the power sharing and competition between the modes is the displacement in wavelength of the steady-state peak gain from the nearest Fabry-Perot mode. The relaxation oscillations and modal competition are shown on a 16mm ciné film in a form that can be readily assessed.

## 1. Introduction

For applications in high bit-rate long-distance optical communications at  $1.55\mu\text{m}$  the semiconductor laser source is required to have a narrow spectral linewidth in order to avoid problems with chromatic dispersion and partition noise. This means that the dynamic spectral broadening<sup>(1)</sup> which occurs under modulation conditions must be avoided as far as possible, and a stable single-longitudinal-mode output is desired at all times. In order to attain this objective many schemes are currently under investigation; these include DFB/DBR laser structures<sup>(2)</sup>, injection locking<sup>(3)</sup>, and the use of external or modified internal cavities with conventional lasers. Whilst significant progress has been achieved with these techniques, a detailed understanding of the mechanisms affecting the transient evolution of laser spectra is still lacking. The objective of the present contribution is to provide such an understanding by the use of a 16mm ciné film of transient spectra produced by computer simulation. The film shows the development of the spectrum during the first few nanoseconds of operation together with the variation of electron concentration in the device, thus providing insight into the laser behaviour in a form which may be readily assessed.

The transient evolution of the laser spectrum has been calculated from numerical solution of the multimode rate equations including the effects of spontaneous emission into the modes. The results show the characteristic relaxation oscillations in each mode together with the competition effects between the modes which occur with a rather slower time scale. The principal parameter which determines this modal competition is the displacement in wavelength of the equilibrium peak gain from the adjacent Fabry-Perot mode<sup>(6)</sup>. In section 2 we describe briefly the models used for the lasing processes, in section 3 results are given showing the temporal development of photon and electron populations, and in section 4 the significance of the above-mentioned wavelength displacement is discussed.

## 2. Rate equations

We use the multimode rate equations<sup>(7)</sup> for a laser structure with a built-in lateral waveguide, neglecting diffusion and assuming spatially uniform photon and electron populations in the active region. We include spontaneous emission coupling into the lasing mode in the form  $\Gamma R_{sp}$  where  $\Gamma$  is the optical confinement factor,  $R_{sp}$  is the total spontaneous emission rate, and  $\beta$  is the wavelength-dependent spontaneous emission factor.  $\beta$  and gain at each mode wavelength are calculated from a simple model<sup>(8)</sup> assuming band-to-band recombination between parabolic bands with no k-selection and with an effective bandgap energy accounting for the bandgap shrinkage effect. The model allows us to express stimulated and spontaneous emission rates in an analytical form via approximations due to Marinelli<sup>(9)</sup> and Joyce and Dixon<sup>(10)</sup>. The total spontaneous emission rate  $R_{sp}$  is given by  $Bnp$  where  $n$  and  $p$  are the electron and hole concentrations, respectively, in the active region, and  $B$  is a constant estimated to have the value  $2 \times 10^{-10} \text{ cm}^3 \text{ s}^{-1}$  for  $1.55\mu\text{m}$  lasers.

The internal loss in quaternary lasers is larger than in GaAs because of the intervalence band absorption<sup>(11)</sup>. Therefore we include a carrier-concentration-dependent loss term in the expression for the photon lifetime in the cavity. The calculated threshold electron concentration for  $200\mu\text{m}$  long, undoped  $\text{In}_{0.59}\text{Ga}_{0.41}\text{As}_{0.88}\text{P}_{0.12}$  laser is about  $1.3 \times 10^{18} \text{ cm}^{-3}$ , and the free carrier absorption at this level (assuming  $n=p$ ) amounts to  $\sim 60 \text{ cm}^{-1}$ , which is approximately equal to the mirror loss. With the diffraction loss in passive layers estimated as  $30 \text{ cm}^{-1}$  and  $\Gamma = 0.67$  we obtain the cavity lifetime equal to  $1.1 \text{ ps}$ .

We consider a rectangular current pulse applied to a laser biased below the threshold. As a first step in the process of solving the multimode rate equations we find the stationary solution for the pulse current in

order to establish the longitudinal mode which dominates at the end of the pulse. In the calculations reported here the rate equations are solved for 15 longitudinal modes, with the ultimately dominant mode situated near the centre of the mode spectrum.

Initial conditions for the transient evolution are determined by solving the stationary multimode rate equations at the pre-bias current. Then a variable stepsize extrapolation method with controlled accuracy, developed by Bulirsch and Stoer<sup>(12)</sup>, is applied to find the transient response to the step pulse current. With the simple model for gain function described above the numerical calculation of the transient development of 15 modes over  $1 \text{ ns}$  requires less than  $7 \text{ s}$  of computing time on a CDC 7600 machine.

## 3. Calculated temporal behaviour

Let us take an example of a  $1.55\mu\text{m}$  laser with an undoped active layer of thickness  $0.3\mu\text{m}$ , stripe width  $5\mu\text{m}$  and cavity length  $200.1\mu\text{m}$ . The threshold current density obtained from the model explained above is approximately  $2 \text{ kA/cm}^2$ . We consider the transient response of this laser, pre-biased at 90% of threshold ( $1.8 \text{ kA/cm}^2$ ), to a step pulse current of 50% above threshold ( $3 \text{ kA/cm}^2$ ). The time evolution of the total single-mirror output power of 15 modes together with that of three strongest modes is illustrated in Fig.1.

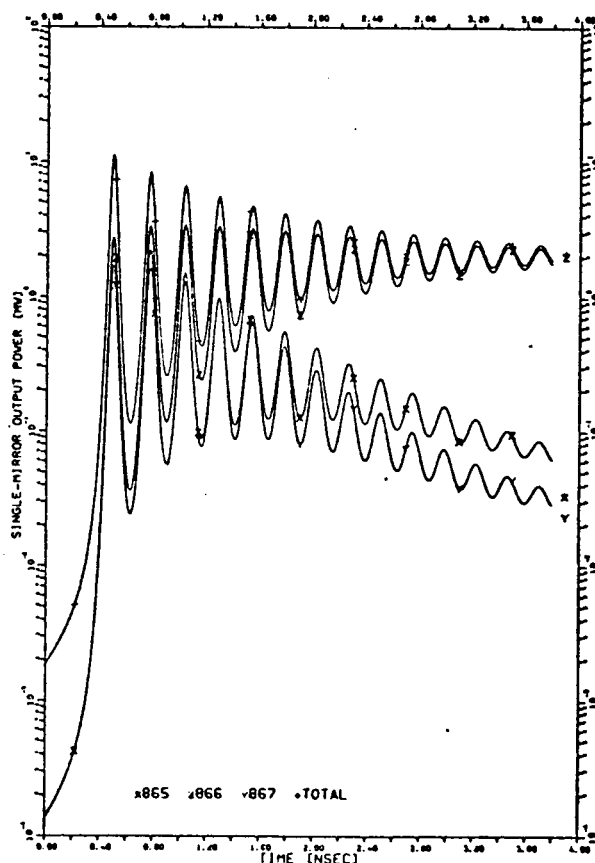


Fig. 1

In order to facilitate their identification, the curves are marked with symbols. The same symbols appearing at the right hand side of the figure represent the stationary values when equilibrium is reached. The modes are labelled at the bottom of the figure by their longitudinal mode numbers which increase with increasing photon energy. On the background of relaxation oscillations with the period  $\sim 250 \text{ ps}$  one can see the flow of power between the modes that occurs within a longer time-scale. It is easier to follow the mode power exchange by looking at the time-averaged spectra as shown in Fig. 2 for five modes. The photon density in Fig. 2 has been averaged for each mode over time interval between adjacent maxima and minima of the rapidly oscillat-

ing photon population, and the results are marked by respective symbols. It can be seen that the shorter-

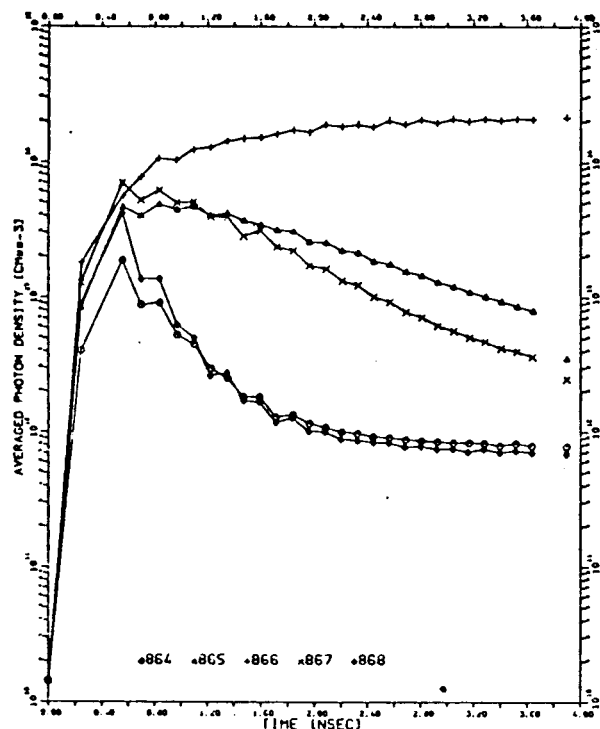


Fig. 2

wavelength mode. 867 tends to dominate at the beginning of oscillations, when the overshoot of the electron concentration at the first spike shifts the gain peak towards shorter wavelength, but is suppressed during the second spike and finally comes third. This is the behaviour of a device that we would call a single-mode laser, since in the stationary state the photon density for the dominant mode is ~500 times greater than that for the adjacent one.

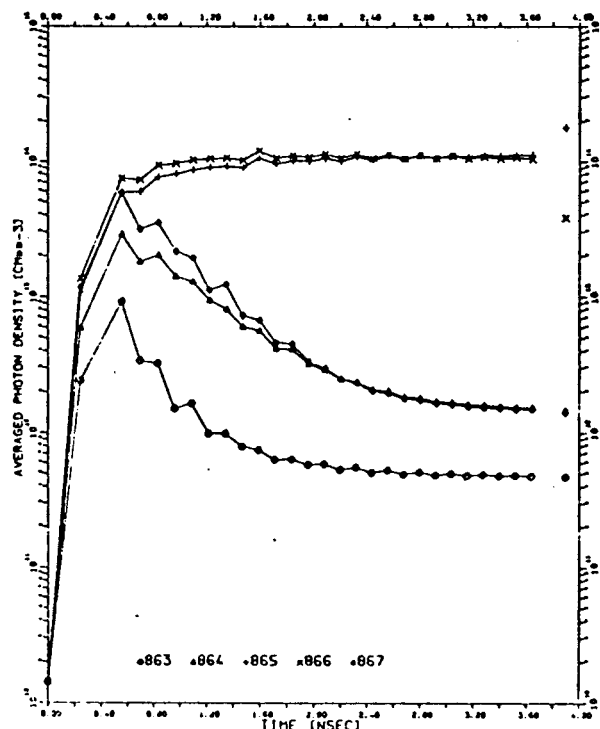


Fig. 3

A very different picture is obtained when the resonator length is changed slightly. Fig.3 illustrates

the situation for a 200.02μm long laser with all other parameters kept the same as previously. Now the power exchange between the strongest modes is much slower and the shorter wavelength mode dominates for as long as 3 ns to become only five times weaker than the dominant mode in the steady state. This represents then a double-mode laser. The reason for such a remarkable difference in the spectra of apparently similar lasers as those in Figs. 2 and 3 is discussed in section 4.

The transient development of laser spectra will be illustrated by a 16 mm ciné-film showing oscillations of electron concentration and photon densities. The layout of the film frame is exemplified in Fig.4. The top left-hand-side plot shows the time dependence of

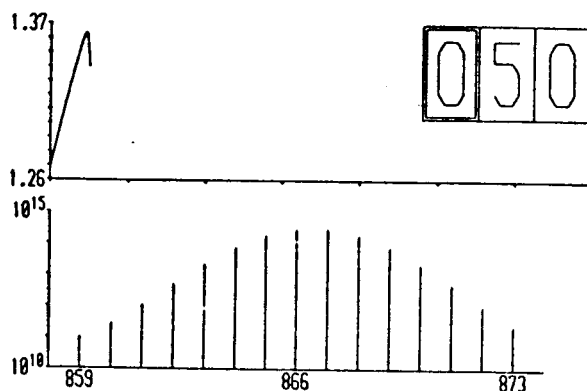


Fig. 4

the electron concentration  $n$  with the  $n$  axis described in units of  $10^{18} \text{ cm}^{-3}$ . The current time in tens of picoseconds is displayed on the right hand side, with the double window marking full nanoseconds. The lower plot represents photon densities of 15 modes plotted on a logarithmic scale. The longitudinal numbers of the central and side modes are given below the plot. The plot is given in terms of mode number rather than wavelength in order to avoid the added complexity resulting from the dynamic wavelength shift (13).

Fig. 4, obtained with the same parameters as Fig. 1, shows a broad spectrum that is excited near the top of the first photon-density spike. As time proceeds the laser spectrum narrows and the relaxation oscillations are damped. The single-mode spectrum of the same laser developed after 3.8 ns is illustrated in Fig.5.

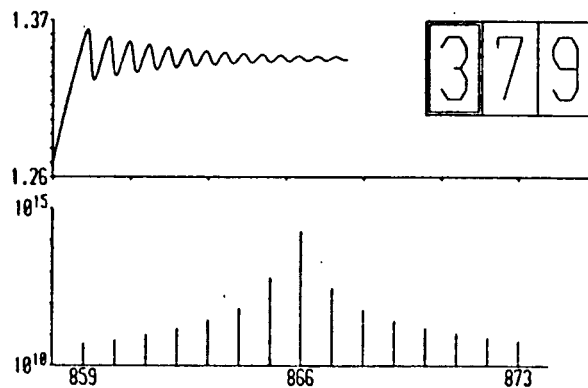


Fig. 5

#### 4. Discussion

Transient evolution of the mode spectra depends dramatically on a very subtle phenomenon, i.e. the position of the gain peak related to the mode wavelengths. During oscillations the gain peak shifts towards shorter wavelength when the electron concentration exceeds its threshold value and vice-versa. The crucial factor is how the gain peak is situated with regard to the dominant mode in the steady-state (final) condition. If the gain peak lies on the longer wavelength side of the

dominant mode then it is relatively easy for this mode to retain its dominant position during oscillations. On the other hand, if the gain peak is placed on the shorter wavelength side, the next (shorter wavelength) mode tends to dominate at the beginning of oscillations and weakens only when the amplitude of electron concentration variations becomes insufficient to shift the gain peak close enough to its wavelength. The competition between the two modes becomes more pronounced as the gain peak in the steady state shifts further towards the next (shorter wavelength) mode. Also the spectral purity in the steady-state is determined mainly by the position of the gain peak, with the maximum purity when the dominant mode wavelength coincides with the gain peak. These properties of the transient solution can be properly described only when the gain peak shift with varying electron concentration is included. In a model with a fixed position of the gain peak all modes would oscillate around their steady state intensity and no changes of the average intensity would occur.

Our calculated values for the shift of peak gain indicate a variation of  $\sim 3.1$  nm for a carrier concentration swing of 2.7% peak-to-valley about the steady state value, which corresponds to that shown in Fig.5. For a  $1.55 \mu\text{m}$  laser of length  $200 \mu\text{m}$  this is equivalent to over 2 mode spacings. In addition to this effect we must also take account of the dynamic wavelength shift<sup>(13)</sup> of the Fabry-Perot modes which arises as a consequence of the refractive-index dependence on the electron concentration<sup>(7)</sup>. The largest reported value of this shift for quaternary lasers, that due to Turley<sup>(14)</sup>, would imply a mode wavelength change of  $0.4$  nm for the carrier concentration swing quoted above. Note that both the peak gain change and the dynamic wavelength shift will be in the same direction with variation of carrier concentration. Thus the net shift of gain peak relative to the mode wavelength is brought down to  $2.7$  nm which is just below 2 mode spacings. Hence in a sense the dynamic wavelength shift helps to mitigate somewhat the influence of gain shift in discouraging single-mode behaviour.

Experimentally, unless special set-ups for mode control are made, controlling the single-mode operation is very difficult because the position of the gain peak can be influenced by temperature or pulse-current-amplitude fluctuations. Recently Henning and Frisch<sup>(15)</sup> have reported true time-resolved measurements showing the considerable magnitude of pulse-to-pulse variation in the spectrum encountered in practice. These effects can be simply modelled by considering small changes in the resonator length. The longitudinal mode spacing can be written in terms of the photon energy:

$$\delta E = \frac{\hbar c}{L \bar{\mu}_{\text{eff}}} \quad (1)$$

with  $L$  as the resonator length and  $\bar{\mu}_{\text{eff}}$  as the effective group index<sup>(7)</sup>. A shift of the energy of the mode  $M$  by  $\delta E/M$  can be achieved by decreasing the cavity length by

$$\Delta L = \frac{L \mu_{\text{eff}}}{m \bar{\mu}_{\text{eff}}} \quad (2)$$

where  $\mu_{\text{eff}}$  is the effective phase index. For  $m = 2$ ,  $M = 866$ ,  $\bar{\mu}_{\text{eff}} = 4.22$ ,  $\mu_{\text{eff}} = 3.34$  and  $L = 200 \mu\text{m}$  we get  $\Delta L = 0.09 \mu\text{m}$ . Such small variations of the cavity length are unavoidable in practice; therefore one can expect that for this reason alone seemingly identical lasers under identical working conditions would demonstrate different transient behaviour:

Now we can come back to the numerical examples given in section 3. A clue to the explanation of different behaviour shown in Figs. 2 and 3 can be found in Table 1, containing the steady-state gain of the longer-wavelength (-1) and shorter-wavelength (+1) modes expressed as a percentage of the dominant-mode gain. It is clear that the peak gain in the laser  $200.1 \mu\text{m}$  long is situated close to the dominant mode on its

longer wavelength side, which is the optimum condition for a single-mode laser. By decreasing the cavity length by  $0.08 \mu\text{m}$  we shift the mode spectrum towards shorter wavelength by nearly half the mode spacing, while the position of the gain peak remains almost unchanged. This way we create a situation where the gain peak is almost half the mode spacing away from the dominant mode and situated on its shorter-wavelength side, which strongly encourages double-mode operation.

Table 1

Cavity length ( $\mu\text{m}$ )	Relative gain (%)	
	Mode -1	Mode +1
200.1	99.88	99.81
200.02	99.71	99.99

## 5. Conclusions

With the aid of a simple analytical model for gain the multimode rate equations for photon and electron concentrations are solved numerically and lasing spectra calculated at each fixed time step of  $4$  ps. The results obtained indicate that one should expect a large variety of transient spectra even from a single laser under modulation conditions, as the evolution of laser spectra is very sensitive to slightest changes in the position of the gain-peak relative to the dominant mode wavelength. The evolution of spectra during the first few nanoseconds of laser operation is illustrated by means of a  $16$  mm ciné-film. The ability to show, at the same time, the transient behaviour of the electron concentration in the active layer of the device, means that effects such as the shift of dominant mode can be demonstrated and readily understood in an intuitive fashion.

## 6. Acknowledgments

The authors express their gratitude to A.G. Steventon and I.D. Henning for numerous helpful discussions and to S.E.H. Turley for making available to us Ref. 14 prior to its publication. Support of British Telecom Research Laboratories is gratefully acknowledged.

## References

1. T. Ikegami, First European Conference on Optical Fibre Communications, London, 16-18 Sept., 1975.
2. F. Koyama, A. Arai, Y. Suematsu and K. Kishino, Electronics Letters, **17**, 938 (1981).
3. D.J. Malyon, D.W. Smith and R.W. Berry, Paper ME5, Third International Conference on Integrated Optics and Optical Fibre Communication, San Francisco, 27-29 Apr., 1981.
4. K.R. Preston, K.C. Woollard and K.H. Cameron, Electronics Letters, **17**, 931 (1981).
5. S. Wang, H.K. Choi and I.H.A. Fattah, IEEE Journal QE-18, 610 (1982).
6. M.J. Adams and M. Osinski, IEE Proceedings Part I, submitted for publication, December 1982.
7. G.H.B. Thompson, Physics of Semiconductor Devices, Wiley, Chichester 1980.
8. M. Osinski and M.J. Adams, IEE Proceedings Part I, submitted for publication, December 1982.
9. F. Marinelli, Solid-State Electronics, **8**, 939 (1965).
10. W.B. Joyce and R.W. Dixon, Applied Physics Letters, **31**, 354 (1977).
11. M. Asada, A.R. Adams, K.E. Stubkjaer, Y. Suematsu, Y. Itaya and S. Arai, IEEE Journal QE-17, 611 (1981).

12. R. Bulirsch and J. Stoer, Numerische Mathematik, 8, 1 (1966).

13. K. Kishino, S. Aoki and Y. Suematsu, IEEE Journal QE-18, 343 (1982)

14. S.E.H. Turley, Electronics Letters, submitted for publication 1982.

15. I.D. Henning and D.A. Frisch, Electronics Letters, 18, 465 (1982).